Degradation and Recovery of *n*-Type Multi-Crystalline Silicon Under Illuminated and Dark Annealing Conditions at Moderate Temperatures

Carlos Vargas, Shuai Nie, Daniel Chen, Catherine Chan, Brett Hallam, Gianluca Coletti, and Ziv Hameiri

***Abstract*—Recently, an *n*-type multi-crystalline silicon (mc-Si) was observed to be susceptible to degradation under illumination at elevated temperatures with similarities to carrier-induced degradation in *p*-type mc-Si. In this study, we demonstrate degradation and regeneration of the effective lifetime of non-diffused *n*-type mc-Si wafers using illuminated and dark annealing conditions at moderate temperatures. Under illuminated annealing conditions, the degradation and regeneration rates of the *n*-type mc-Si are observed to be slower than those of the *p*-type mc-Si; however, the opposite trend was observed under dark annealing conditions. The carrier-induced degradation kinetics of the *n*-type wafers can be described by degradation and regeneration that occur simultaneously, and the activation energies have been identified to be 1.23 ± 0.16 eV for the degradation process and 1.34 ± 0.08 eV for the regeneration. Surprisingly, no degradation was observed in *n*-type mc-Si under dark annealing above 160 °C. Rather, at these conditions, a two-stage improvement in the lifetime was observed. Although degradation occurs after a subsequent laser treatment, the stable lifetime at the end of the degradation is still slightly higher than its initial value.**

***Index Terms*—Degradation, multi-crystalline silicon (mc-Si), *n*-type, silicon solar cells.**

I. Introduction

MULTI-CRYSTALLINE silicon (mc-Si) wafers are known to degrade under illumination at elevated temperature [1]–[8] and under dark annealing [9]–[12]. This degradation is often named light and elevated temperature induced degradation (LeTID) [2], [3], [5], [13], [14]; however, as it has been reported that light is not required for its formation, is also called carrier-induced degradation (CID) [2], [5], as it seems that excess carriers are the main requirement for this degradation. Other forms of light-induced degradation, such as the formation of the boron–oxygen (B–O) complex or iron–boron (Fe–B) pair dissociation, cannot explain this degradation of carrier lifetime, as CID has been observed also in gallium-doped mc-Si wafers, and its time scales are significantly slower compared with B–O degradation [1]. Under standard field operation conditions, the degradation and recovery cycle of CID in *p*-type mc-Si solar cells has an extremely long timescale from 5 to 20 years, depending on the location of the photovoltaic (PV) system [2], and would result in a significant energy yield loss over this period (because of a drop in efficiency of up to 16% relative) [15]. The shift of the silicon (Si) PV industry toward passivated emitter rear cells (PERC) fabricated using *p*-type mc-Si substrates [16] is being challenged by this degradation. To date, the root cause of CID has not been clarified and, therefore, remains a key area of research focus.

Krauss *et al*. suggested that the rear surface passivation plays a role in the formation of CID [6]. However, the evidence presented by Nakayashiki *et al*. [4] demonstrated that CID is caused by a bulk defect, as a reduction of the bulk lifetime (τ_{bulk}) was observed after light soaking at elevated temperature. This conclusion was later confirmed by Vargas *et al*. [17] who reported no degradation of the surface passivation quality provided by different silicon nitride (SiN_x) layers when degrading wafers using the laser-accelerated process proposed of Payne *et al*. [3]. Padmanabhan *et al*. [18] supported the hypothesis of a bulk defect being the root cause of CID as they observed degradation and regeneration of both PERC and aluminum back surface field cells. Based on these reports, several studies have been focused on extracting the Shockley–Read–Hall parameters of the CID-related bulk defect using the injection-dependent lifetime spectroscopy [19] technique [4], [7], [20], [21]. Tungsten (W), titanium (Ti), and molybdenum (Mo) were suggested as possible defect candidates; however, later studies suggested that these should be ruled out because of their low diffusivity being inconsistent with observed results [22], [23].

Generally, the CID defect in mc-Si is activated by illumination at elevated temperature [2], [24]. However, Chan *et al*. [9] demonstrated that CID can also be activated by dark annealing at moderate temperatures. Later reports by Chen *et al*. [10] and Fung *et al*. [11] demonstrated that degradation caused by dark annealing alone is similar to that caused by illumination at

Manuscript received September 9, 2018; revised November 5, 2018; accepted December 3, 2018. This work was supported by the Australian Government through the Australian Renewable Energy Agency under Project 2017/RND001. *(Carlos Vargas and Shuai Nie contributed equally to this work.) (Corresponding author: Shuai Nie.)*

C. Vargas, S. Nie, D. Chen, C. Chan, B. Hallam, and Z. Hameiri are with the School of Photovoltaic and Renewable Energy Engineering, University of New South Wales, Sydney, NSW 2052, Australia (e-mail: c.vargascastrillon@student.unsw.edu.au; s.nie@unsw.edu.au; daniel.chen@unsw.edu.au; catherine.chan@unsw.edu.au; brett.hallam@unsw.edu.au; ziv.hameiri@gmail.com).

G. Coletti is with the School of Photovoltaic and Renewable Energy Engineering, University of New South Wales, Sydney, NSW 2052, Australia, and also with the ECN Part of TNO, Petten 1755 ZG, The Netherlands (e-mail: coletti@ecn.nl).

Color versions of one or more of the figures in this paper are available online at http://ieeexplore.ieee.org.

Digital Object Identifier 10.1109/JPHOTOV.2018.2885711

elevated temperature. Fung *et al*. [11] suggested that dark annealing processes allow defect precursors to move into mc-Si bulk and then to gradually deplete. Recently, Vargas *et al*. [12] studied the degradation and regeneration of *p*-type mc-Si in the dark; they found that higher temperatures lead to faster degradation and regeneration rates, as well as a smaller degradation extent. Based on the extracted rates, they reported activation energies of 1.08 ± 0.05 eV and 1.11 ± 0.04 eV for the degradation and regeneration processes, respectively.

The CID kinetics is of particular importance as it can provide insight into the nature of the defect. Bredemeier *et al*. [25] studied the CID kinetics by using two exponential functions associated with the fast and slow defects. However, they only considered the degradation part of the degradation/regeneration curve. A single exponential function and an improved double exponential function were then used by Kwapil *et al*. [26] to extract the CID kinetics. They found that the degradation rate is almost linearly proportional to the excess minority carrier concentration Δn. Vargas *et al*. [12] then used a modified two exponents model to describe the CID kinetics by considering that the degradation and regeneration happen simultaneously [26]. A good agreement was achieved between the model and the experimental data.

It is important to note that almost all the studies agree that a high-temperature firing process is required to trigger the CID [5], [7], [8], [27]. Several recent studies have suggested that hydrogen, introduced during firing step, plays a role in CID of mc-Si wafers [4], [9], [10], [17], [23], [27]–[29]. It can either form a part of the CID defect complex [27], [29] or passivate the recombination active defect [29], [30]. Kersten *et al*. demonstrated that the CID was only observed on fired samples with a hydrogen-containing dielectric layer, such as hydrogenated-SiN_x [31]. Vargas *et al.* modulated the extent of CID degradation by varying the hydrogen fraction in SiN_x layers [17]; an increasing extent of degradation was observed by increasing the hydrogen released from the dielectric layer during the firing. Additionally, a thicker SiN_x layer was shown to cause a more severe CID [32]. Recently, Jensen *et al.* [33] reported that they were able to separate the effects of the thermal process (firing) from the introduction of hydrogen into the wafer. They found that the firing process itself is not required for CID to occur; the introduction of hydrogen via a plasma source is able to trigger degradation.

Currently, little is known regarding CID mechanism in *n*-type wafers. Sio *et al*. [34] reported a degradation and regeneration in *n*-type mc-Si wafers with phosphorous diffusion under illumination at elevated temperatures using samples fired at a peak temperature of 700 °C. They observed a smaller degradation extent and slower degradation and regeneration rates compared with *p*-type mc-Si wafers that were treated under similar conditions. In that study, degradation was only observed in the *n*-type wafers that were fired. This particular behavior is similar to CID of *p*-type mc-Si wafers, which as discussed has a strong dependence on the firing conditions and has not been observed for non-fired samples [5], [7], unless hydrogen is introduced into the Si in another manner [33]. Although not using mc-Si, Chen *et al*. [35] studied CID on *n*-type Czochralski (Cz) grown wafers. They observed bulk degradation on a fired sample with a diffused layer (either boron or phosphorus) and surface degradation on fired non-diffused samples. Since CID in mc-Si *n*-type wafers was only studied under illumination in [34], in this contribution, both accelerated laser-based process [3] and dark annealing are used to study the degradation and regeneration of non-diffused *n*-type mc-Si wafers. A direct comparison is done with *p*-type mc-Si wafers treated under similar conditions. A detailed investigation of the temperature dependence of degradation and recovery under dark annealing is presented. We also determine the kinetics of the different processes using our modified double-exponential model [12].

II. Material and Method

Six sister 6-in phosphorus-doped *n*-type (thickness: 207 ± 4 μm; doping density N_D: $(1.0 \pm 0.1) \times 10^{15}$ cm^{-3}) and six boron-doped *p*-type (thickness: 184 ± 5 μm; doping density N_A: $(8.5 \pm 0.4) \times 10^{15}$ cm^{-3}) commercially available high-performance mc-Si wafers were used in this study. All wafers underwent saw damage etching (3 μm per side) using hydrofluoric acid, acetic acid, and nitric acid at room temperature. After receiving a Radio Corporation of America cleaning, SiN_x layers with refractive index of 2.08 (at 632 nm) and thickness of 75 nm were deposited on all wafers by an industrial plasma-enhanced chemical vapor deposition system (MAiA, Meyer Burger) [36] to form symmetrical lifetime test structures. Five wafers (from each polarity) were then fired at a set peak temperature of 855 °C (actual wafer peak temperature of 774 ± 9 °C), followed by a laser cleaving into square tokens with dimension 3.9 cm $\times$ 3.9 cm. Sets of six sister tokens (*p*- and *n*-type) were selected to be used in this study.

One set from each polarity (five fired tokens and one non-fired token) went to laser-accelerated degradation at a wafer temperature of 140 °C and light intensity of 45 kW/m^2 [3] in progressive treatment time steps until a completed degradation and regeneration cycle was achieved. The evolution of the effective lifetime $\tau_{\rm eff}$ was monitored after each treatment step using PL images (BTi LIS-R1) [37] and a photoconductance-based lifetime tester (WCT-120, Sinton instruments) [38]. The $\tau_{\rm eff}$ measurements were done at a sample temperature of 30 °C and were analyzed using the generalized method [39].

The effect of dark annealing at moderate temperatures was investigated using another set of six *n*-type tokens (five fired and one non-fired) and *in situ* lifetime measurements using a WTC-120TS lifetime tester (Sinton instruments). The following actual wafer temperatures (as measured by a *k*-type thermocouple in direct contact with a similar sample) were investigated: 100, 120, 140 (fired and un-fired tokens), 150, and 160 °C. An additional token from a neighboring location to this set was dark annealed at 175 °C. One set of *p*-type tokens (three fired and one non-fired) received the same dark annealing process at 140, 150, and 175 °C.

In this study, the Kane–Swanson [40] method, as implemented in the Sinton Instrument spreadsheet, was used to monitor changes in the surface saturation current density (J_{0s}) and the high-injection $\tau_{\rm bulk}$ at $\Delta n = 1 \times 10^{16}$ cm^{-3} (for *n*-type) and

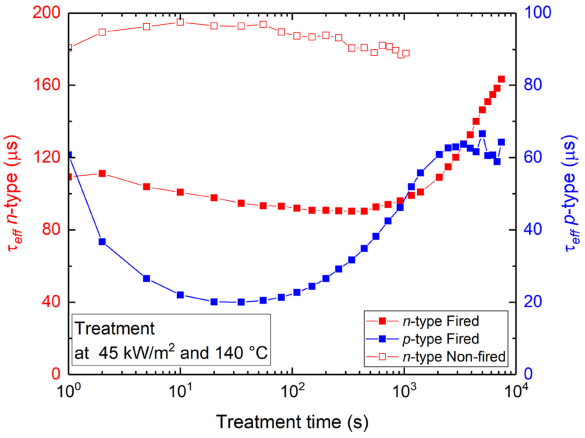

Fig. 1. Evolution of the effective lifetime as a function of the laser processing time. The lines are an aid for the reader and the state before treatment corresponds to a time of 1 s.

$\Delta n = 3 \times 10^{16}$ cm^{-3} (for p-type). Quokka 2 [41] based one-dimensional modeling was used to confirm the obtained values by varying J_{0s} and τ_{Bulk} to fit the measured τ_{eff}. As Auger lifetime seems to be almost constant between room temperature and 200 °C [42], the Auger model of Richter *et al.* [43] was used in this study for all the analysis. The normalized defect density (NDD) was calculated using the following equation, based on the high injection τ_{bulk} (τ_{bulk} is used here to avoid impacts by changes in the surface passivation quality):

$$\mathrm{NDD}\,(t) = \left[\frac{1}{\tau_{\mathrm{Bulk}}\,(t)} - \frac{1}{\tau_{\mathrm{bulk}}\,(t=0)}\right]. \qquad (1)$$

In this study, the CID kinetics was obtained using the following equation [12]:

$$\begin{aligned}\mathrm{NDD}\,(t) &= \mathrm{NDD}_{\max}\left[1-\exp\left(-r_{\deg}t\right)\right] \\ &\quad - \mathrm{NDD}_{\max}\,(1+A)\left[1-\exp\left(-r_{\mathrm{reg}}t\right)\right] \qquad (2)\end{aligned}$$

where $\mathrm{NDD}_{\max}$ is the maximum value of the NDD, $r_{\deg}$ (r_{reg}) is the degradation (regeneration) rate, and A is a correction factor to account for additional improvements of τ_{bulk} at the end of the process. The fitting was made using the 95% confidence bounds method, as implemented in MATLAB [44].

III. Results and Discussion

A. Accelerated Laser Degradation and Mitigation of the Degradation of n-Type mc-Si

The evolution of the τ_{eff} (extracted at $\Delta n = 1 \times 10^{15}$ cm^{-3}) of representative n-type and p-type wafers after firing is presented in Fig. 1 as a function of the cumulated laser treatment duration. The initial lifetimes of the fired samples were 110 ± 6 μs and 60 ± 3 μs for the n-type and p-type wafers, respectively. Both types of wafers demonstrated degradation and recovery of τ_{eff}. Fig. 1 also shows the normalized lifetime of the non-fired n-type wafer (initial lifetime of 180 ± 9 μs). No degradation and recovery can be identified for this wafer (τ_{eff} variations below 8.5%), pointing toward a CID behavior, similar to a previous study [24]. However, there are clear differences between the wafers. 1) The degradation rate of the n-type wafers during illuminated annealing is much slower than that of the p-type wafers. The maximum degradation is obtained after 35 s for the p-type wafers, while it takes 150 s of laser treatment to reach maximum degradation of the n-type wafers. 2) The extent of the degradation is much smaller (∼17%) for the n-type wafers compared with the p-type wafers (∼77%). 3) τ_{eff} of the n-type wafers improves considerably (>50% and still improving) at the end of the laser treatment carried out here, in contrast to the p-type wafers that demonstrate a moderate improvement in the range of 5%–10%.

To further illustrate the degradation and recovery in the n-type wafers, Fig. 2(a) presents the injection-dependent τ_{eff} after different laser treatment time durations. The change in the low injection region indicates a strong bulk-related degradation. In order to confirm this hypothesis, J_{0s} and the high-injection τ_{bulk} were extracted using two methods: 1) the slope-based method of Kane–Swanson [40] at $\Delta n = 1 \times 10^{16}$ cm^{-3}; and 2) fitting of the measured τ_{eff} using Quokka 2 (in Δn range of 5.4×10^{15} cm^{-3} to 1.7×10^{16} cm^{-3}) [41]. Both methods show similar trends, as illustrated in Fig. 2(b): 1) a clear bulk degradation, followed by a significant improvement after a long laser-based treatment; and 2) improvement in surface passivation quality (as indicated by about 14% reduction of J_{0s}). The absolute difference between the obtained J_{0s} is probably because of the non-uniform Δn profile across the wafer's depth, as discussed in [45]. Both trends confirm that the observed degradation is within the bulk. The increase of τ_{bulk} at the end of the process is likely because of hydrogen passivation of preexisting bulk defects or a reduction of the firing-induced CID-related defect [46]. Note that contrary to [47] and [48], we observe improvement of the surface passivation quality during light and moderate temperature treatments, probably because of the different light sources (laser used in this study) and different $\mathrm{SiN_x}$ layers used in this study.

Fig. 3 presents PL images of both n- and p-type wafers at different laser treatment stages. All the images were taken with an exposure time of 0.3 s using an 810 nm laser and photon flux of 2.55×10^{17} cm^{-2}s^{-1}. The images were processed using the recently developed software described in [49]. The relative change in PL intensity of the images was calculated by $(I–I_0)/I_0 \times 100\%$, where I_0 and I are the PL images before the treatment and at the most degraded or final state. As shown in Fig. 3, degradation and regeneration occurs across the entire wafer, but not uniformly. While it seems that grain boundaries and other crystal defects degrade less than the intra-grain regions in the p-type wafers [50], we have not identified a correlation between the degradation extent and particular locations in the n-type wafers. This will be investigated more deeply in the near future.

B. Degradation and Recovery of n-Type mc-Si Under Dark Annealing

The evolution of the normalized τ_{bulk} extracted at $\Delta n = 1 \times 10^{16}$ cm^{-3} following the Kane–Swanson method [40] for the n-type wafers under dark annealing at different temperatures is

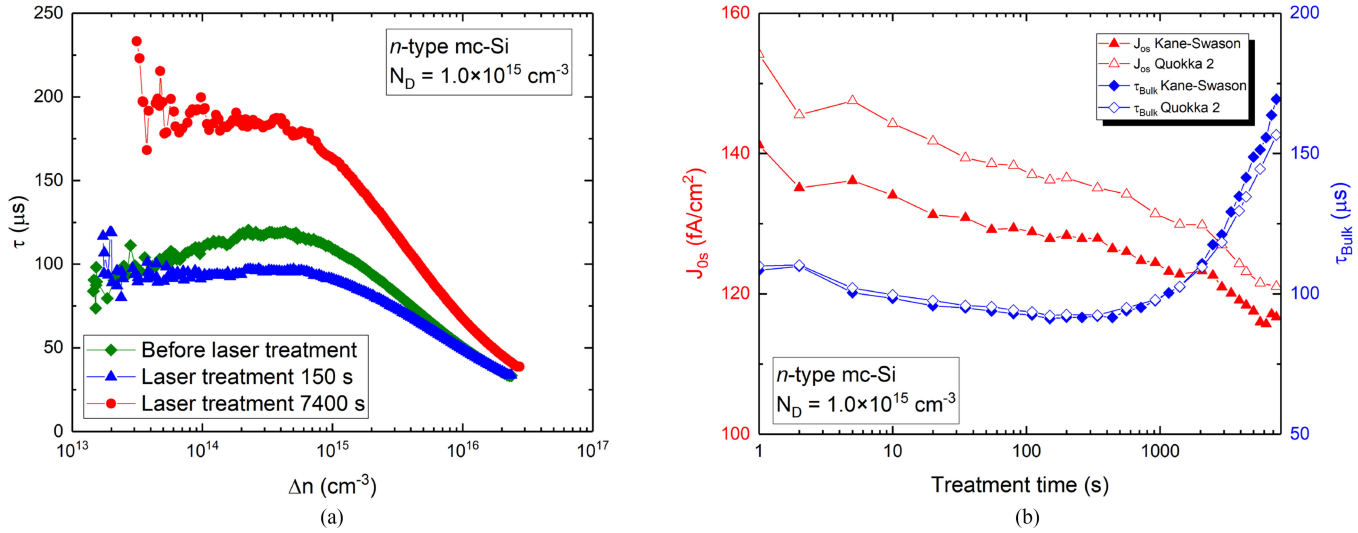

Fig. 2. (a) Injection-dependent effective lifetime of an *n*-type wafer as a function of the laser treatment time duration. (b) Surface saturation current density and high injection bulk lifetime as extracted using the Kane–Swanson [40] method and Quokka 2 [41] modeling.

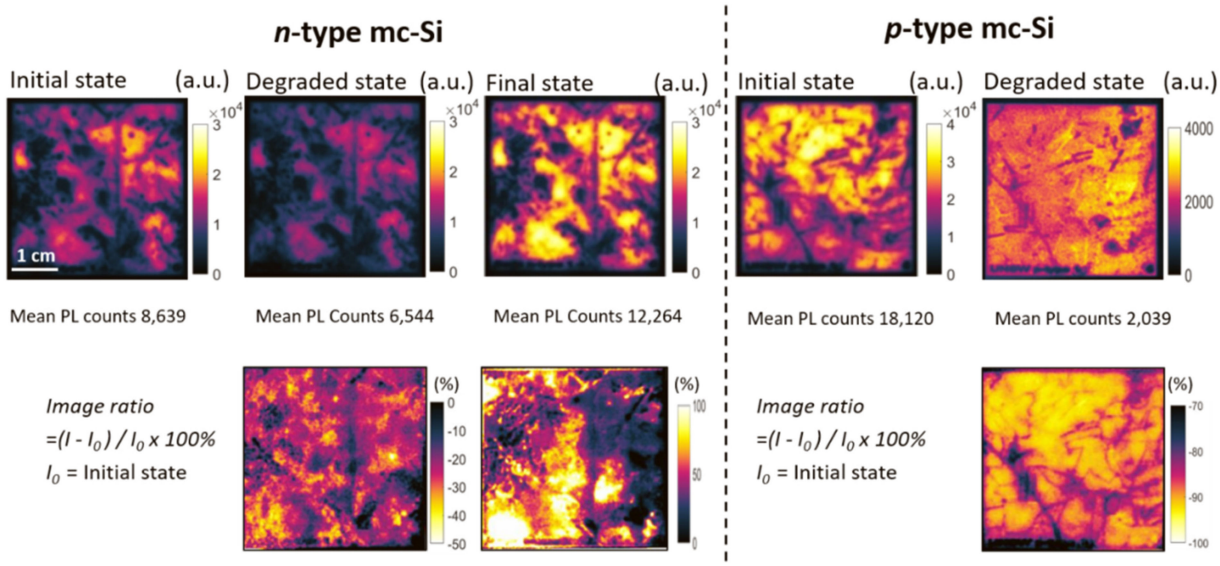

Fig. 3. PL images for the *n*- and *p*-type mc-Si samples at different stages along with the image ratio compared with the state before the laser process. Note the different scales between the images.

shown in Fig. 4(a). A slight change in the J_{0s} was observed (<5%) during the process. $\tau_{\rm bulk}$ measured at room temperature is in the range 102 ± 16 μs for the fired *n*-type wafers and 201 ± 10 μs for the non-fired wafer. The $\tau_{\rm bulk}$ of the *n*-type wafer reduced 49% after firing (the surface passivation is not degraded after firing) in contrast to the *p*-type wafer where lifetime improvement was observed after the firing process. This can be explained by competing processes happening during firing: improvement of bulk due to hydrogenation and degradation due to CID. However, at this stage, we cannot separate these possible processes. The time evolution of the normalized $\tau_{\rm bulk}$ at $\Delta n = 3 \times 10^{16}$ cm^{-3} of the *p*-type samples (initial lifetime 131 ± 6 μs for the fired wafers; and 72 ± 4 μs for the non-fired one) is displayed in Fig. 4(b). Since the degradation and regeneration of these samples are very slow at temperatures below 175 °C [12], only partial regeneration was observed in the time frame of this experiment. Note that the Kane–Swanson method [40] was used to extract $\tau_{\rm bulk}$ for the dark annealed wafers as Quokka 2 [41] cannot be used for fitting lifetime measurements at higher temperatures. Based on the comparison between the two methods at room temperature, we assume that the obtained trend is a good representation, despite the fact that the *p*-type wafers were not measured at high injection.

For the *n*-type wafers [see Fig. 4(a)], degradation and regeneration of $\tau_{\rm bulk}$ can be appreciated, except for annealing at 160 and 175 °C, where only an improvement is observed. Higher degradation extent is obtained for *n*-type wafers treated at lower temperatures. The degradation extent is decreasing with

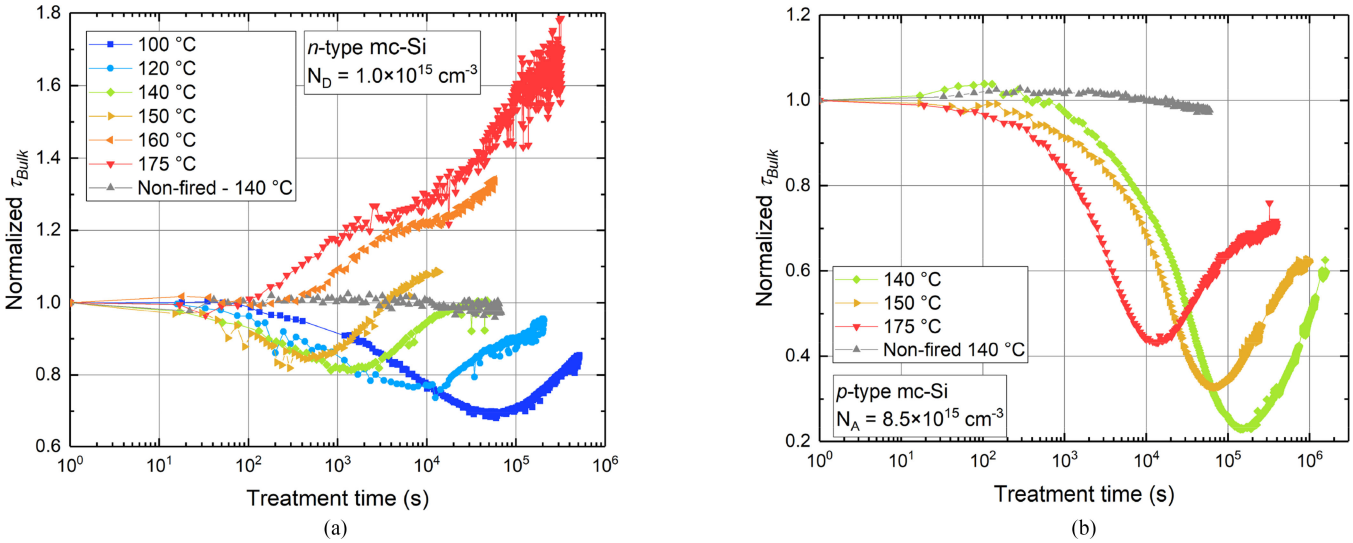

Fig. 4. Evolution of the high injection bulk lifetime for wafers under dark annealing at different temperatures. (a) n-type wafers. (b) p-type wafers.

increasing annealing temperature. The degradation rate has also a strong dependence on the temperature; at higher temperatures, the degradation rate is much faster. No degradation and regeneration of $\tau_{\rm bulk}$ can be seen for the non-fired wafer. A similar behavior is observed for the p-type wafers (see Fig. 4(b) and [12]), however, with slower degradation and regeneration rates compared with the n-type wafers and with a larger degradation extent. Interestingly, the $\tau_{\rm bulk}$ values of n-type wafers are higher at the end of the annealing process above 150 °C compared with their initial values. A similar observation was reported for p-type samples [12]. We assume that it is due to passivation of preexisting bulk defects or preformed CID defects during firing. Further studies are required to prove this hypothesis. To our knowledge, this is the first time that degradation of the n-type mc-Si wafers using dark annealing is reported. The similarities between the n- and p-type wafers (temperature dependence of the degradation extend and rates) may indicate that the defect responsible for the degradation is the same in both materials.

Surprisingly, the $\tau_{\rm bulk}$ of n-type wafer keeps improving under dark annealing at 175 °C. In order to test the stability of this improvement, a wafer was processed using the accelerated laser process at 45 kW/m^2 and 140 °C for almost 2 h at the end of 90 h dark annealing treatment at 175 °C (this laser condition is roughly equivalent to 20 years in the field which is similar to the lifespan of PV modules). Despite the fact that $\tau_{\rm bulk}$ was degraded to about 50% of its post dark annealing value (see Fig. 5), the stable $\tau_{\rm bulk}$ at the end of the degradation (105 μs) is still slightly higher than the lifetime before dark annealing (92 μs). This indicates that dark annealing at 175 °C (or higher temperature) can suppress the lifetime degradation (from its initial value after firing) because of CID in the n-type mc-Si wafers. It is interesting to note the higher degradation extent and very slow rates observed during this laser treatment, compared with the wafers with no pre-dark annealing (see Fig. 1). This difference could be an indication of modulation of the degradation kinetics due to initial dark annealing as suggested by Chan *et al.* [10] for the p-type mc-Si.

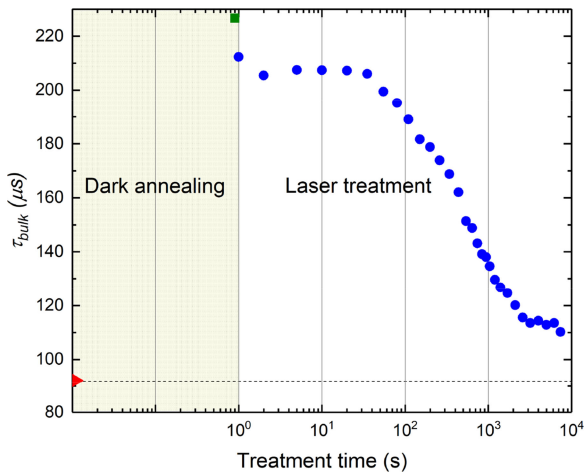

Fig. 5. Evolution of the high injection $\tau_{\rm bulk}$ under laser treatment for the wafer that initially received dark annealing at 175 °C.

C. Kinetics and Activation Energies of the Illuminated and Dark Annealing Degradation and Recovery Reactions

The evolution of the NDD is analyzed using the proposed kinetic model [see (2)] for the wafers under the laser-accelerated degradation process (see Fig. 1) and the wafers under dark annealing (except for 160 and 175 °C), where the degradation and regeneration are assumed to occur simultaneously. Good agreement between the measurements and the model was obtained for the wafers under laser treatment [see Fig. 6(a)]. In the case of dark annealing, excellent fits are obtained for all temperatures, except for the wafer annealed at 100 °C [see Fig. 6(b)].

Table I presents the degradation and regeneration rates of wafers treated by laser illumination (45 kW/m^2 and 140 °C) and dark annealing at 140 °C, based on the fit to the proposed model [see (2)]. The data for p-type (treated by dark annealing) is obtained from [12], as the degradation and regeneration are too slow to observe in the time frame of this experiment. For laser-based treatments, the rates of the p-type wafers are

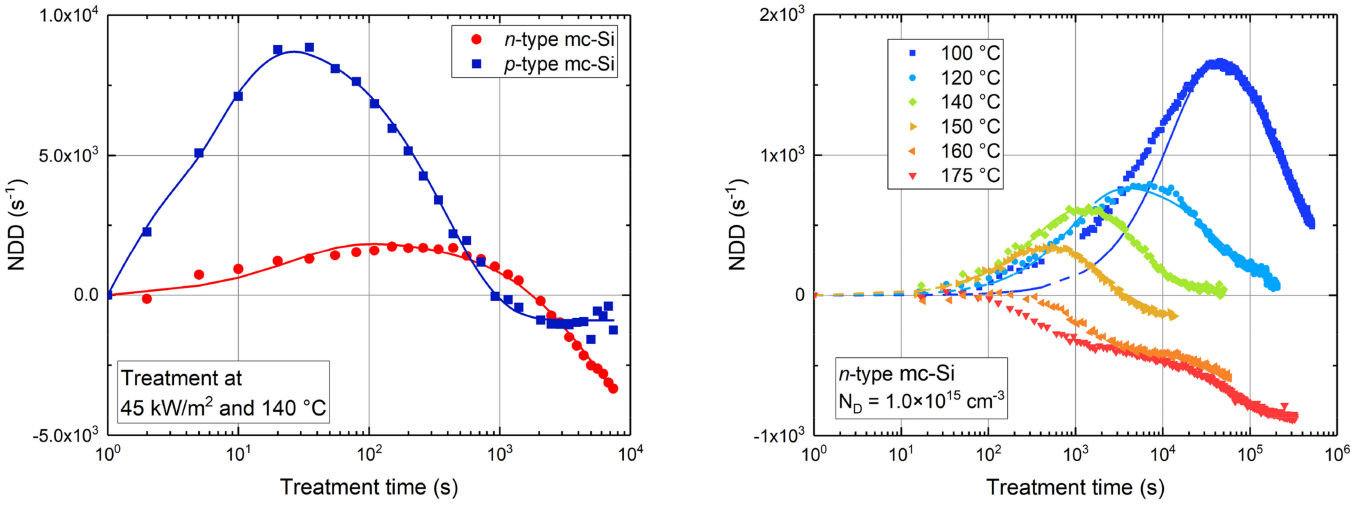

Fig. 6. Measured (symbols) and modeled (solid lines) NDD. (a) *n*- and *p*-type wafers under laser-based treatment. (b) *n*-type wafers under dark annealing (NDD of the sample under the dark annealing at 160 and 175 °C was also included without fit).

TABLE I
DEGRADATION AND REGENERATION RATES OF SOME SAMPLES BASED ON THE PROPOSED FITTING MODEL (FIT AT 140 °C)

Sample	NDD_{max} (s^{-1})	A	r_{deg} (s^{-1})	r_{reg} (s^{-1})
p-type mc-Si – Laser treatment	$(9.55 \pm 0.38) \times 10^3$	0.093 ± 0.018	0.153 ± 0.020	$(2.61 \pm 0.24) \times 10^{-3}$
p-type mc-Si – Dark annealing at 138 °C [12]	$(3.85 \pm 0.16) \times 10^4$	-0.059 ± 0.021	$(5.52 \pm 0.43) \times 10^{-6}$	$(4.54 \pm 0.46) \times 10^{-7}$
n-type mc-Si – Laser treatment	$(2.01 \pm 0.23) \times 10^3$	2.7 ± 1.1	0.038 ± 0.018	$(1.81 \pm 0.75) \times 10^{-4}$
n-type mc-Si – Dark annealing at 140 °C	$(7.81 \pm 0.29) \times 10^2$	-0.047 ± 0.010	$(2.56 \pm 0.20) \times 10^{-3}$	$(1.67 \pm 0.12) \times 10^{-4}$

faster than those of the *n*-type wafers (five times faster degradation rate, more than ten times faster regeneration rate). This observed behavior parallels that observed by Sio *et al.* [34] on mc-Si *p*-type and *n*-type wafers under illumination. However, an opposite trend is obtained under dark annealing, with the rates of degradation and regeneration for *n*-type wafers being faster than those of the *p*-type wafers. A plausible reason is one that was explored earlier in [35] suggesting that the recovery of CID may be related to the out-diffusion of a hydrogen species toward the surface of the wafer. It is also plausible that if hydrogen is involved in the formation of the recombination active defect, then the diffusion of hydrogen to the defect precursor may also play a role in determining the degradation rate.

At 150 °C, the reported diffusivity of H^- is approximately 2.5 orders of magnitude higher than that of H^+. Furthermore, the reported diffusivity of H^0 is approximately 1.5 orders of magnitude higher than that of H^- [51]. Under dark annealing conditions in *n*-type Si at 140 °C, the fractional charge state concentrations of H^+, H^0, and H^- are 6.4×10^{-2}, 7.8×10^{-4}, and 9.4×10^{-1}, respectively, with a clear dominance of H^- [52]. In contrast, in *p*-type Si, the corresponding fractional charge state concentrations are 1×10^0, 6.8×10^{-8} and 1.5×10^{-10}, respectively. This gives a domination of H^- in *n*-type Si and domination of H^+ in *p*-type Si. Furthermore, the fractional concentration of H^- is 9.5 orders of magnitude higher in *n*-type Si than that in *p*-type Si. Similarly, the fractional concentration of H^0 is approximately four orders of magnitude higher in *n*-type Si than that in *p*-type Si. Under these conditions, one would then expect both the degradation and regeneration rates in *n*-type to be several orders of magnitude greater than in *p*-type in the dark.

Under illumination, the expected Δn of the *n*-type and *p*-type samples from the initial state to the most degraded state are approximately 5.4×10^{16} to 5.2×10^{16} cm^{-3} and 8.0×10^{16} to 5.8×10^{16} cm^{-3}, respectively. For these carrier concentrations, the expected fractional hydrogen charge state concentrations in the *n*-type for H^+, H^0, and H^- are 7.1×10^{-1}, 2.7×10^{-1}, and 1.4×10^{-2}, respectively. Since the change of Δn during the laser treatment is small (4%), the fractional concentrations remain the same. For *p*-type, the corresponding concentrations at initial state are 6.8×10^{-1} (H^+), 3.1×10^{-1} (H^0), and 1.4×10^{-2} (H^-). Then, the concentration for H^0 and H^- decreases by 12% and 15%, respectively, during treatment, while the fractional concentration for H^+ increases by 6%. For both *n*-type and *p*-type under laser treatment, H^+ (with the lowest diffusivity among three) is dominant for both *n*-type and *p*-type. We cannot confidently pinpoint the relationship between hydrogen diffusion and fast degradation and regeneration rates of the *p*-type wafer under illumination.

For both *n*-type and *p*-type wafers, the degradation rate under illumination is faster than that obtained using dark annealing. For *n*-type, the degradation rate increased by a factor of

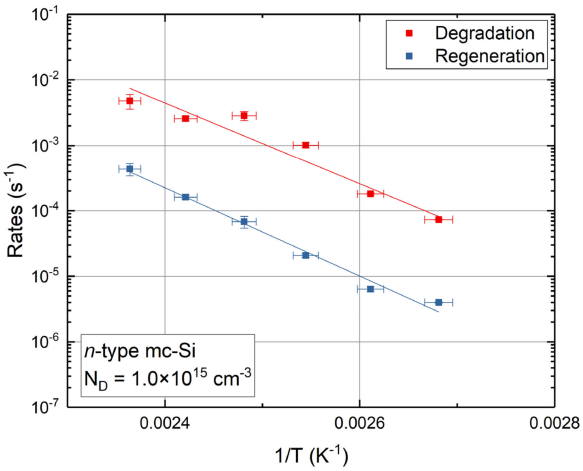

Fig. 7. Arrhenius plot of the samples under dark annealing with the best linear fit.

15 under illumination compared with dark annealing. This closely correlates with the expected increase in the total electron concentration of the sample under illumination compared with that during dark annealing. For *p*-type, the degradation rate increased by a factor of 2.7×10^4 under illumination. This also closely correlates with the expected increase in the total electron concentration. The acceleration of both degradation and regeneration rates with illumination on *p*-type wafers has been explored in various works [10], [23], [26]. CID has been understood to be dependent on the carrier concentration and possibly even thermally generated carriers. Thus, an increase in illumination may drive forward both the degradation and regeneration reactions.

Interestingly, we find the regeneration rates of *n*-type wafers treated by laser and dark annealing to be comparable, with no significant increase in the regeneration rate with illumination. This unexpected result cannot yet be explained and requires further investigation and modeling, and could potentially provide more clues in determining the mechanism for regeneration, such as a reducing concentration of H^- with carrier injection. It is also interesting to note that the ratios from *n*-type to *p*-type for the degradation or regeneration rate under the dark treatment are both around 400. Regarding the laser treatment, the ratios from *n*-type to *p*-type are 0.25 for the degradation rate and 0.07 for the regeneration rate. This indicates that the CID mechanisms are different between *n*-type and *p*-type under illumination. The large value of the factor *A* for the *n*-type wafer under the laser treatment indicating that the improvement of τ_{eff} at the end of the process is significant.

Based on the extracted rates for the samples under dark annealing [see Fig. 6(b)], the activation energies were extracted using an Arrhenius analysis, as illustrated in Fig. 7. The Arrhenius function was defined as

$$r_{\text{deg/reg}} = C \times \exp\left[-\frac{E_{\text{deg/reg}}}{k_B T}\right] \tag{3}$$

where C is a constant, k_B is the Boltzmann constant, T is the temperature, and $E_{\text{deg/reg}}$ are the degradation and regeneration activation energies, respectively. The activation energies are found to be 1.23 ± 0.16 eV for the degradation process and 1.34 ± 0.08 eV for the regeneration process. These energies are similar to those determined for *p*-type mc-Si wafers (1.04 ± 0.06 eV for the degradation process and 1.05 ± 0.04 eV for the regeneration process [12]). The small difference (in the range of 20%) could be explained by the smaller temperature range used in this paper (100–150 °C, limited by the temperatures at which degradation is observed in the *n*-type mc-Si) compared with the wider range (140–300 °C) used in [12] for *p*-type wafers, which can lead to an additional uncertainty in the confidence intervals for the *n*-type samples. The fact that the degradation kinetics under the laser and dark annealing of *n*- and *p*-type wafers can be modeled using the same equation could be an indication of a similar degradation mechanism.

IV. Conclusion

In this study, the presence of a minority-carrier-lifetime degradation and regeneration cycle in non-diffused and fired *n*-type mc-Si wafers was demonstrated by using accelerated laser-based illuminated and dark annealing at moderate temperatures. The degradation rate and degradation extent are found to be lower than those of *p*-type mc-Si wafers when the illuminated annealing is used, similar to previously reported results. Surprisingly, the *n*-type mc-Si treated by dark annealing has a faster degradation and regeneration rate than the *p*-type mc-Si under same treatment; however, the extent is smaller, and the degradation cannot be observed at annealing temperatures of 160 °C or above. Significant lifetime improvement of the *n*-type wafers is observed under higher temperature (above 160 °C) dark annealing; however, the improved lifetime is not stable under a subsequent accelerated laser degradation process. Instead, a pronounced and slower degradation was found on that wafer, indicating a possible modulation of the degradation kinetics due to dark annealing. Based on a model that considers degradation and regeneration happening simultaneously, the evolution of those processes in *n*-type mc-Si can be described, and based on the extracted rates, activation energies are 1.23 ± 0.16 eV for the degradation process and 1.34 ± 0.08 eV for the regeneration process. Considering the similitudes found for the *n*-type and *p*-type mc-Si samples processed under similar conditions (firing, laser-accelerated process, dark annealing, and kinetics), it is very likely that both have similar nature; therefore, the *n*-type mc-Si also suffers from the same CID that occurs in *p*-type mc-Si. These findings could help guide further studies to determine the root causes of degradation of mc-Si as well as possible mitigation solutions.

Acknowledgment

The views expressed herein are not necessarily the views of the Australian Government, and the Australian Government does not accept responsibility for any information or advice contained herein. The authors would like to thank the Solar Industrial Research Facility team at UNSW for their help in the fabrication of the samples used in this study.

REFERENCES

[1] K. Ramspeck *et al.*, "Light induced degradation of rear passivated mc-Si solar cells," in *Proc. 27th Eur. Photovolt. Sol. Energy Conf. Exhib.*, 2012, pp. 861–865, doi: 10.4229/27thEUPVSEC2012-2DO.3.4.

[2] F. Kersten *et al.*, "Degradation of multicrystalline silicon solar cells and modules after illumination at elevated temperature," *Sol. Energy Mater. Sol. Cells*, vol. 142, pp. 83–86, 2015, doi: 10.1016/j.solmat.2015.06.015.

[3] D. N. R. Payne *et al.*, "Acceleration and mitigation of carrier-induced degradation in *p*-type multi-crystalline silicon," *Phys. Status Solidi, Rapid Res. Lett.*, vol. 10, no. 3, pp. 237–241, Mar. 2016, doi: 10.1002/pssr.201510437.

[4] K. Nakayashiki *et al.*, "Engineering solutions and root-cause analysis for light-induced degradation in *p*-type multicrystalline silicon PERC modules," *IEEE J. Photovolt.*, vol. 6, no. 4, pp. 860–868, Jul. 2016, doi: 10.1109/JPHOTOV.2016.2556981.

[5] C. E. Chan *et al.*, "Rapid stabilization of high-performance multicrystalline *p*-type silicon PERC cells," *IEEE J. Photovolt.*, vol. 6, no. 6, pp. 1473–1479, Nov. 2016, doi: 10.1109/JPHOTOV.2016.2606704.

[6] K. Krauss, F. Fertig, D. Menzel, and S. Rein, "Light-induced degradation of silicon solar cells with aluminiumoxide passivated rear side," *Energy Procedia*, vol. 77, pp. 599–606, 2015, doi: 10.1016/j.egypro.2015.07.086.

[7] D. Bredemeier, D. Walter, S. Herlufsen, and J. Schmidt, "Lifetime degradation and regeneration in multicrystalline silicon under illumination at elevated temperature," *AIP Adv.*, vol. 6, 2016, Art. no. 035119, doi: 10.1063/1.4944839.

[8] D. Bredemeier, D. Walter, S. Herlufsen, and J. Schmidt, "Understanding the light-induced lifetime degradation and regeneration in multicrystalline silicon," *Energy Procedia*, vol. 92, pp. 773–778, Aug. 2016, doi: 10.1016/j.egypro.2016.07.060.

[9] C. Chan *et al.*, "Modulation of carrier-induced defect kinetics in multicrystalline silicon PERC cells through dark annealing," *Sol. RRL*, vol. 1, Feb. 2017, Art. no. 1600028, doi: 10.1002/solr.201600028.

[10] D. Chen *et al.*, "Evidence of an identical firing-activated carrier-induced defect in monocrystalline and multicrystalline silicon," *Sol. Energy Mater. Sol. Cells*, vol. 172, pp. 293–300, Dec. 2017, doi: 10.1016/j.solmat.2017.08.003.

[11] T. H. Fung *et al.*, "Impact of annealing on the formation and mitigation of carrier-induced defects in multi-crystalline silicon," *Energy Procedia*, vol. 124, pp. 726–733, 2017, doi: 10.1016/j.egypro.2017.09.087.

[12] C. Vargas, G. Coletti1, C. Chan, D. Payne, and Z. Hameiri, "On the impact of dark annealing and room temperature illumination on *p*-type multicrystalline silicon wafers," *Sol. Energy Mater. Sol. Cells*, vol. 189, pp. 166–174, 2018.

[13] A. Zuschlag, D. Skorka, and G. Hahn, "Degradation and regeneration analysis in mc-Si," in *Proc. Conf. Rec. IEEE Photovolt. Spec. Conf.*, Nov. 2016, pp. 1051–1054, doi: 10.1109/PVSC.2016.7749772.

[14] A. Herguth, C. Derricks, P. Keller, and B. Terheiden, "Recovery of LeTID by low intensity illumination: Reaction kinetics, completeness and threshold temperature," *Energy Procedia*, vol. 124, pp. 740–744, 2017, doi: 10.1016/j.egypro.2017.09.090.

[15] K. Petter *et al.*, "Dependence of LeTID on brick height for different wafer suppliers with several resistivities and dopants," in *Proc. 9th Int. Workshop Crystalline Silicon Sol. Cells*, 2016, vol. 6, pp. 1–17.

[16] M. A. Green, "The passivated emitter and rear cell (PERC): From conception to mass production," *Sol. Energy Mater. Sol. Cells*, vol. 143, pp. 190–197, Dec. 2015, doi: 10.1016/j.solmat.2015.06.055.

[17] C. Vargas *et al.*, "Influence of silicon nitride and its hydrogen content of carrier-induced degradation in multicrystalline silicon," in *Proc. 33rd Eur. Photovolt. Sol. Energy Conf. Exhib. Amsterdam*, 2017, pp. 561–564.

[18] M. Padmanabhan *et al.*, "Light-induced degradation and regeneration of multicrystalline silicon Al-BSF and PERC solar cells," *Phys. Status Solidi, Rapid Res. Lett.*, vol. 10, no. 12, pp. 874–881, Dec. 2016, doi: 10.1002/pssr.201600173.

[19] S. Rein, *Lifetime Spectroscopy: A Method of Defect Characterization in Silicon for Photovoltaic Applications*. New York, NY, USA: Springer, 2005.

[20] A. E. Morishige *et al.*, "Lifetime spectroscopy investigation of light-induced degradation in *p*-type multicrystalline silicon PERC," *IEEE J. Photovolt.*, vol. 6, no. 6, pp. 1466–1472, Nov. 2016, doi: 10.1109/JPHOTOV.2016.2606699.

[21] C. Vargas *et al.*, "Recombination parameters of lifetime-limiting carrier-induced defects in multicrystalline silicon for solar cells," *Appl. Phys. Lett.*, vol. 110, no. 9, Feb. 2017, Art. no. 092106, doi: 10.1063/1.4977906.

[22] M. A. Jensen *et al.*, "Solubility and diffusivity: important metrics in the search for the root cause of light-and elevated temperature-induced degradation," *IEEE J. Photovolt.*, vol. 8, no. 2, pp. 448–455, Mar. 2018, doi: 10.1109/JPHOTOV.2018.2791411.

[23] T. Niewelt *et al.*, "Understanding the light-induced degradation at elevated temperatures: Similarities between multicrystalline and floatzone *p*-type silicon," *Prog. Photovolt. Res. Appl.*, vol. 26, no. 8, pp. 533–542, Aug. 2018, doi: 10.1002/pip.2954.

[24] D. N. R. Payne *et al.*, "Rapid passivation of carrier-induced defects in *p*-type multi-crystalline silicon," *Sol. Energy Mater. Sol. Cells*, vol. 158, pp. 102–106, Dec. 2016, doi: 10.1016/j.solmat.2016.05.022.

[25] D. Bredemeier, D. Walter, and J. Schmidt, "Light-induced lifetime degradation in high-performance multicrystalline silicon: Detailed kinetics of the defect activation," *Sol. Energy Mater. Sol. Cells*, vol. 173, pp. 2–5, Dec. 2017, doi: 10.1016/j.solmat.2017.08.007.

[26] W. Kwapil, T. Niewelt, and M. C. Schubert, "Kinetics of carrier-induced degradation at elevated temperature in multicrystalline silicon solar cells," *Sol. Energy Mater. Sol. Cells*, vol. 173, pp. 80–84, Dec. 2017, doi: 10.1016/j.solmat.2017.05.066.

[27] R. Eberle, W. Kwapil, F. Schindler, M. C. Schubert, and S. W. Glunz, "Impact of the firing temperature profile on light induced degradation of multicrystalline silicon," *Phys. Status Solidi, Rapid Res. Lett.*, vol. 10, no. 12, pp. 861–865, Dec. 2016, doi: 10.1002/pssr.201600272.

[28] A. Wenham *et al.*, "Hydrogen-induced degradation," in *Proc. 7th World Conf. Photovolt. Energy Convers.*, Jun. 2018, pp. 1–8.

[29] M. A. Jensen, A. E. Morishige, J. Hofstetter, D. B. Needleman, and T. Buonassisi, "Evolution of *p*-type LeTID defects in multicrystalline silicon during degradation and regeneration," *IEEE J. Photovolt.*, vol. 7, no. 4, pp. 980–987, Jul. 2017, doi: 10.1109/JPHOTOV.2017.2695496.

[30] D. Bredemeier, D. C. Walter, and J. Schmidt, "Possible candidates for impurities in mc-Si wafers responsible for light-induced lifetime degradation and regeneration," *Sol. RRL*, vol. 2, Dec. 2017, Art. no. 1700159, doi: 10.1002/solr.201700159.

[31] F. Kersten, J. Heitmann, and J. W. Müller, "Influence of Al_2O_3 and SiN_x passivation layers on LeTID," *Energy Procedia*, vol. 92, pp. 828–832, Aug. 2016, doi: 10.1016/j.egypro.2016.07.079.

[32] U. Varshney *et al.*, "Influence of dielectric passivation layer thickness on LeTID in multicrystalline silicon," in *Proc. 7th World Conf. Photovolt. Energy Convers.*, Jun. 2018, pp. 363–367.

[33] M. A. Jensen *et al.*, "Evaluating root cause: The distinct roles of hydrogen and firing in activating light- and elevated temperature-induced degradation," *J. Appl. Phys.*, vol. 124, no. 8, Aug. 2018, Art. no. 085701, doi: 10.1063/1.5041756.

[34] H. C. Sio *et al.*, "Light and elevated temperature induced degradation in *p*-type and *n*-type cast-grown multicrystalline and mono-like silicon," *Sol. Energy Mater. Sol. Cells*, vol. 182, pp. 98–104, Aug. 2018, doi: 10.1016/j.solmat.2018.03.002.

[35] D. Chen *et al.*, "Hydrogen induced degradation: A possible mechanism for light- and elevated temperature-induced degradation in *n*-type silicon," *Sol. Energy Mater. Sol. Cells*, vol. 185, pp. 174–182, Oct. 2018, doi: 10.1016/j.solmat.2018.05.034.

[36] Z. Hameiri *et al.*, "Low-absorbing and thermally stable industrial silicon nitride films with very low surface recombination," *IEEE J. Photovolt.*, vol. 7, no. 4, pp. 996–1003, Jul. 2017, doi: 10.1109/JPHOTOV.2017.2706424.

[37] T. Trupke, R. A. Bardos, M. C. Schubert, and W. Warta, "Photoluminescence imaging of silicon wafers," *Appl. Phys. Lett.*, vol. 89, no. 4, Jul. 2006, Art. no. 044107, doi: 10.1063/1.2234747.

[38] R. A. Sinton, A. Cuevas, and M. Stuckings, "Quasi-steady-state photoconductance, a new method for solar cell material and device characterization," in *Proc. 25th Photovolt. Spec. Conf.*, May 1996, pp. 457–460, doi: 10.1109/PVSC.1996.564042.

[39] H. Nagel, C. Berge, and A. G. Aberle, "Generalized analysis of quasi-steady-state and quasi-transient measurements of carrier lifetimes in semiconductors," *J. Appl. Phys.*, vol. 86, no. 11, pp. 6218–6221, Dec. 1999, doi: 10.1063/1.371633.

[40] D. Kane and R. Swanson, "Measurement of the emitter saturation current by a contactless photoconductivity decay method," in *Proc. 18th IEEE Photovolt. Spec. Conf.*, Jan. 1985, vol. 18, pp. 578–583.

[41] A. Fell, K. R. McIntosh, M. Abbott, and D. Walter, "Quokka version 2: Selective surface doping, luminescence modeling and data fitting," in *Proc. 23rd Photovolt. Sci. Eng. Conf.*, 2013, pp. 1–4.

[42] S. Wang and D. MacDonald, "Temperature dependence of Auger recombination in highly injected crystalline silicon," *J. Appl. Phys.*, vol. 112, no. 11, Dec. 2012, Art. no. 113708, doi: 10.1063/1.4768900.

[43] A. Richter, S. W. Glunz, F. Werner, J. Schmidt, and A. Cuevas, "Improved quantitative description of Auger recombination in crystalline silicon," *Phys. Rev. B, Condens. Matter Mater. Phys.*, vol. 86, no. 16, pp. 1–14, Oct. 2012, doi: 10.1103/PhysRevB.86.165202.

[44] MathWorks, "PDF documentation for curve fitting toolbox." [Online]. Available: https://au.mathworks.com/help/pdf_doc/curvefit/index.html. [Accessed on: Apr. 9, 2018].

[45] R. Dumbrell, M. Juhl, T. Trupke, and Z. Hameiri, "Extracting metal contact recombination parameters from effective lifetime data," *IEEE J. Photovolt.*, vol. 8, no. 6, pp. 1413–1420, Nov. 2018, doi: 10.1109/JPHOTOV.2018.2861761.

[46] L. J. Geerligs *et al.*, "Precipitates and hydrogen passivation at crystal defects in *n*- and *p*-type multicrystalline silicon," *J. Appl. Phys.*, vol. 102, no. 9, Nov. 2007, Art. no. 093702, doi: 10.1063/1.2800271.

[47] D. Sperber, A. Graf, D. Skorka, A. Herguth, and G. Hahn, "Degradation of surface passivation on crystalline silicon and its impact on light-induced degradation experiments," *IEEE J. Photovolt.*, vol. 7, no. 6, pp. 1627–1634, Nov. 2017, doi: 10.1109/JPHOTOV.2017.2755072.

[48] K. Kim *et al.*, "Degradation of Surface Passivation and Bulk in *p*-type Monocrystalline Silicon Wafers at Elevated Temperature," *IEEE J. Photovolt.*, pp. 1–9, 2018, doi: 10.1109/JPHOTOV.2018.2878791.

[49] D. N. R. Payne, C. Vargas, Z. Hameiri, S. R. Wenham, and D. M. Bagnall, "An advanced software suite for the processing and analysis of silicon luminescence images," *Comput. Phys. Commun.*, vol. 215, pp. 223–234, Jun. 2017, doi: 10.1016/j.cpc.2017.02.012.

[50] T. Luka, S. Großer, C. Hagendorf, K. Ramspeck, and M. Turek, "Intra-grain versus grain boundary degradation due to illumination and annealing behavior of multi-crystalline solar cells," *Sol. Energy Mater. Sol. Cells*, vol. 158, pp. 43–49, Dec. 2016, doi: 10.1016/j.solmat.2016.05.061.

[51] D. Mathiot, "Modeling of hydrogen diffusion in *n*-and *p*-type silicon," *Phys. Rev. B*, vol. 40, no. 8, pp. 5867–5870, Sep. 1989, doi: 10.1103/PhysRevB.40.5867.

[52] R. Chen *et al.*, "Impact of the impurity concentration on modulating charge state occupation in silicon," submitted for publication, 2018.

Authors' photographs and biographies not available at the time of publication.